

Chapter 1

Dissipative systems in contact with a heat bath: Application to Andrade creep

Florian Theil, Tim Sullivan, Marisol Koslovski, and Michael Ortiz

The fundamental question addressed in this work is: *How does a dissipative system behave when it is placed in contact with a heat bath?* Specifically, it is desired to derive a variational characterization of the trajectories of the system, i.e., a functional whose minimizers are the system trajectories. For definiteness, consider systems whose state is described by an N -dimensional array $x \in \mathbb{R}^N$ of generalized coordinates. The energetics of the system are described by an energy function $E(t, x)$. The explicit time dependence of E may arise, for example, as a result of the application to the system of a time-dependent external field. In addition, the system is assumed to be *dissipative*, and, therefore, the equilibrium equations are of the form:

$$0 \in \partial_x E(t, x) + \partial \Psi(\dot{x}) \tag{1.1}$$

where Ψ is a dissipation potential. These equilibrium equations define a set of ordinary differential equations which, given appropriate conditions at, say, $t = 0$, can be solved uniquely for the trajectory $x(t)$, $t \geq 0$. If $\Psi(z) = \frac{1}{2}|z|^2$ one obtains the classic gradient flow of the potential E . If Ψ is homogeneous of degree one, then the system becomes rate-independent: i.e., if $x(t)$ solves (1.1)

Florian Theil

Warwick University, Mathematics Institute, Coventry, CV47AL, United Kingdom e-mail: f.theil@warwick.ac.uk

Tim Sullivan

Warwick University, Mathematics Institute, Coventry, CV47AL, United Kingdom e-mail: t.j.sullivan1@warwick.ac.uk

Marisol Koslovski

School of Mechanical Engineering, Purdue University, 585 Purdue Mall West Lafayette, IN 47907-2088, USA e-mail: marisol@purdue.edu

Michael Ortiz

Engineering and Applied Sciences Division, California Institute of Technology Pasadena, CA 91125, USA, e-mail: ortiz@aero.caltech.edu

for E and φ is a reparametrization of time, then $\tilde{x}(t) = x(\varphi(t))$ solves (1.1) for $\tilde{E}(t, \cdot) = E(\varphi(t), \cdot)$. Another direct consequence is the stability requirement

$$\Psi^*(-\partial_x E(t, x)) < \infty, \quad (1.2)$$

where Ψ^* is the Legendre-transform of Ψ . Rigorous analysis and a review of the literature on equation (1.1) in the rate-independent case can be found in [13, 12].

To include the effect of thermal noise we leave the purely deterministic framework and consider stochastic systems where the trajectories are no longer unique but random and define a probability measure on path space. More precisely, as a first step we replace the time-continuum $\{t \geq 0\}$ by a discrete set $0 = t_0 < t_1 < \dots$ of times and consider the Markov chain with transition probability densities proportional to

$$\exp\left(-\left(E(t_{n+1}, x_{n+1}) + |t_{n+1} - t_n| \Psi\left(\frac{x_{n+1} - x_n}{t_{n+1} - t_n}\right)\right) / \varepsilon_n\right).$$

The parameter ε measures the strength of the thermal fluctuations. As a second step we determine the limiting process which is obtained when $\varepsilon_n = \theta(t_{n+1} - t_n)$ and the fineness of the time discretization $h = \sup_n(t_{n+1} - t_n)$ tends to 0. The constant θ is proportional to the temperature, the proportionality constant is not known and has to be estimated by comparing the model predictions with measurements.

In the classical case of linear kinetics, in which $\Psi(z) = \frac{1}{2}|z|^2$, the limiting path-measure is generated by well-known stochastic differential equations. In this paper we will mostly focus on the rate-independent case where Ψ is 1-homogeneous. Here the limiting measure is generated by ordinary differential equations, i.e. the evolution is deterministic. However, the differential equation depends in a nontrivial way on E and Ψ .

As a representative example of application, the theory is applied to the case of Andrade creep in metals; the theory shows that Andrade creep represents the mean-field behavior of an ensemble of linear elastic dislocations moving on a slip plane through a random array of obstacles under the action of an applied resolved shear stress at finite temperature. In order to establish this connection, the energetics and dynamics of the dislocation ensemble are described by means of the Koslowski-Cuitiño-Ortiz phase-field model [10]. The resulting governing equations are simplified by means of a mean-field approximation. The analysis then shows that the slip strain grows as a 1/3 power of time, i.e., the system exhibits Andrade creep.

1.1 Heuristic derivation

We proceed to introduce the basic scheme that accords probabilities to the trajectories of a dissipative system. The first step in the derivation is to discretize the equations of evolution in time and to reinterpret the time-discretized equations as defining the optimal transport of probability measures. An interior-point regularization of the Kantorovich form of the transport problem then effectively places the system in contact with a thermal bath. Conveniently, the regularized incremental problem can be solved explicitly in closed form for the transition probability distribution.

The small-time-step limit is considered in section 1.2.

1.1.1 Heuristic derivation

If the system is conservative, i.e. $\Psi(\dot{x}) \equiv 0$, then the instantaneous state $x(t)$ of the system at time t follows directly from energy minimization, i.e., from the problem:

$$E(t, x(t)) = \inf_{y \in \mathbb{R}^N} E(t, y). \quad (1.3)$$

This variational framework can be extended to dissipative systems by time discretization [15, 16, 17, 13, 12]. Specifically, consider a discrete time incremental process consisting of a sequence of states $x_n \in \mathbb{R}^N$ at times $t_n = nh$, $h > 0$ fixed, and introduce the incremental work function W :

$$W_n(x_n, x_{n+1}) = E(t_{n+1}, x_{n+1}) - E(t_n, x_n) + |t_{n+1} - t_n| \Psi \left(\frac{x_{n+1} - x_n}{t_{n+1} - t_n} \right). \quad (1.4)$$

It should be carefully noted that $W(x_n, x_{n+1})$ is determined by both the *energetics* and the *kinetics* of the system and depends on both the initial and the final configuration of the system over the time step. For a given state x_n the state x_{n+1} is a minimizer of W_n .

The incremental problem above can be re-interpreted as an *optimal transport* problem in which the incremental work function W as defined by (1.4) is regarded as a *cost function*, i.e., as the cost of rearranging the system from one configuration, x_n , to another one, x_{n+1} . Consider the probability density functions $\rho_n: \mathbb{R}^N \rightarrow \mathbb{R}$ describing the state of the system at each time step $t_n = nh$. The corresponding optimal transport problem for the $(n+1)^{\text{th}}$ time step is:

$$\inf \mathcal{F}_h[u], \quad (1.5a)$$

$$\text{subject to: } \int_{\mathbb{R}^N} u(x_n, x_{n+1}) dx_{n+1} = \rho_n(x_n), \quad (1.5b)$$

$$\iint_{\mathbb{R}^N} u(x_n, x_{n+1}) dx_n dx_{n+1} = 1, \quad (1.5c)$$

where $u(x_n, x_{n+1}) = \rho_{n+1}(x_{n+1}|x_n)\rho_n(x_n)$ is the joint probability density of two states x_n and x_{n+1} at successive time steps and

$$\mathcal{F}_h[u] := \iint_{\mathbb{R}^N} W(x_n, x_{n+1})u(x_n, x_{n+1}) dx_n dx_{n+1}. \quad (1.6)$$

In addition, it follows that

$$\rho_{n+1}(x_{n+1}) = \int_{\mathbb{R}^N} u(x_n, x_{n+1}) dx_n. \quad (1.7)$$

Problem (1.5) is a linear programming problem. Introducing Lagrange multipliers $\lambda: \mathbb{R}^N \rightarrow \mathbb{R}$ and $\mu \in \mathbb{R}$, define the Lagrangian

$$\mathcal{L}_h[u] := \mathcal{F}_h[u] + \iint_{\mathbb{R}^N} u(x_n, x_{n+1})\lambda(x_n) dx_n dx_{n+1} + \mu \int_{\mathbb{R}^N} u(x_n, x_{n+1}) dx_n dx_{n+1}. \quad (1.8)$$

In order to model the effect of a heat bath of “temperature” $\varepsilon > 0$, additionally introduce the interior-point regularization:

$$\mathcal{L}_h^\varepsilon[u] := \mathcal{L}_h[u] + \varepsilon \int_{\mathbb{R}^N} u(x_n, x_{n+1}) \log u(x_n, x_{n+1}) dx_n dx_{n+1}. \quad (1.9)$$

The second term on the right-hand side is the negative of the well-known Gibbs-Boltzmann entropy functional for the probability density u , and has the effect of heavily penalizing deterministic, coherent evolutions. The unique minimizer of the extended Lagrangian subject to the constraints (1.5b) and (1.5c) is given by

$$u(x_n, x_{n+1}) = \frac{\rho_n(x_n)}{Z(x_n)} \exp\left(-\frac{W(x_n, x_{n+1})}{\varepsilon}\right), \quad (1.10)$$

where the partition function Z is given by

$$Z(x_n) := \int_{\mathbb{R}^N} \exp\left(-\frac{W(x_n, x_{n+1})}{\varepsilon}\right) dx_{n+1}. \quad (1.11)$$

Finally, (1.7) yields the explicit representation

$$\rho_{n+1}(x_{n+1}) = \int_{\mathbb{R}^N} \frac{\rho_n(x_n)}{Z(x_n)} \exp\left(-\frac{W(x_n, x_{n+1})}{\varepsilon}\right) dx_n. \quad (1.12)$$

Note that, in order for (1.12) to make sense, the work function $W(x_n, x_{n+1})$ must grow rapidly enough as $|x_{n+1}| \rightarrow +\infty$ to ensure that $Z(x_n)$ is finite for each $x_n \in \mathbb{R}^N$. Physically, setting physical temperature $\Theta = \varepsilon/k_B$ in terms of Boltzmann's constant k_B , ε can be interpreted as the temperature of heat bath with which the system is coupled.

From now on $\rho_n^{h,\varepsilon}$ we be interpreted as the transition probability of a Markov chain, i.e.

$$\text{law}(X_{n+1} \mid X_1, \dots, X_n) = \rho_{n+1}^{h,\varepsilon}(\cdot \mid X_n). \quad (1.13)$$

In [18] we give a more extensive discussion together with illustrative examples.

1.2 Mathematical results

We consider the limiting behavior of the Markov-chain (1.13) as h tends to 0 and $\varepsilon = \theta h$, where θ is a temperature-like constant. If the friction potential Ψ is 1-homogeneous, and the potentials E and Ψ are convex and coercive we can characterize the asymptotic behavior completely. It turns out that the limiting process is deterministic and can be obtained as a solution of an ordinary differential equation.

Theorem 1. *Let Ψ be 1-homogeneous, coercive and convex and define*

$$F(v^*) = \log \left\{ \int \mathrm{d}v \exp(-\langle v^*, v \rangle - \Psi(v)) \right\}.$$

Let $X_n^{h,\varepsilon}$ be a realization of the Markov chain (1.13). If $\varepsilon = h$ and E has the property that $F(DE(\cdot, t))$ be convex, then as $h \downarrow 0$, $(X_{[t/h]}^{h,\theta h})$ converges in probability in $L^\infty([0, T], \mathbb{R}^N)$ to the differentiable, deterministic process $y = y^\theta$ satisfying the ordinary differential equation

$$\dot{y} = -\theta DF[D_y E(t, y)], \quad (1.14)$$

where $F(v^) = \log \left\{ \int \mathrm{d}v \exp(-\langle v^*, v \rangle - \Psi(v)) \right\}$. More precisely, for any $T > 0$, $\lambda > 0$,*

$$\mathbb{P} \left[\sup_{0 \leq t \leq T} |X_t^{h,\theta h} - y_t^\theta|_2 \geq \lambda \right] \in O(\sqrt{h}) \text{ as } h \downarrow 0. \quad (1.15)$$

The proof can be found in [18].

Note that $F(v^*) < \infty$ if and only if $\Psi^*(-v^*) < \infty$, i.e. we recover the stability criterion (1.2) although the evolution (1.14) is no longer rate-independent.

In many applications, the dissipation potential Ψ may not be coercive, so that F is infinite everywhere. In some cases the analysis can be carried over, an important application of this generalization of the KCO-model which is discussed in the next chapter.

Corollary 1 (Degenerate friction potential Ψ). *A) Let V be a finite-dimensional vector space and $\Psi : V \rightarrow [0, \infty)$ be given by*

$$\Psi(z) = \sum_i \sigma_i |z_i|$$

where $\sigma_i > 0$ for all $i \in \{1 \dots n\}$. Then

$$F(v^*) = - \sum_i \log(\sigma_i^2 - (v_i^*)^2).$$

B) Let X be another vector space such that V is imbedded into X , $E(t, u)$ be time-dependent, coercive quadratic form on X and the reduced quadratic form $E_{\text{red}} : [0, T] \times V \rightarrow \mathbb{R}$ be defined by

$$E_{\text{red}}(t, \xi) = \min\{E(t, u) \mid \pi(u) = \xi\},$$

where π is the orthogonal projection induced by the imbedding. Then for each $\theta > 0$, $T > 0$, as $h \downarrow 0$ the projection $\pi(X_{[t/h]}^{h, \theta h})$ converges in probability in $L^\infty([0, T]; \mathbb{R}^n)$ to the differentiable, deterministic process $y = y^\theta$ satisfying

$$\dot{y}_t = -\theta DF(D_\xi E_{\text{red}}(t, \xi)). \quad (1.16)$$

The proof can be found in [18].

1.3 Application to crystallographic slip and creep

In this section, the preceding formalism and analysis are applied to *Andrade creep*, also known as β -creep. In 1910, Andrade [1, 2] reported that as a function of time, t , the creep deformation, y , of soft metals at constant temperature and applied stress can be described by a power law $y(t) \sim t^{1/3}$. Similar behavior has been observed in many classes of materials, including non-crystalline materials. Recently, it has been suggested that Andrade creep is an example of critical behavior [5, 6, 7]. In these theories, creep is considered as an instance of critical avalanche formation analogous to sandhill models introduced to explain self-organized criticality. However, creep differs from sandhill behavior in two notable respects: the avalanches are nucleated by thermal activation; and the system exhibits strain hardening. Several numerical simulations are able to predict the power law behavior of the plastic deformation at constant temperature and applied stress in agreement with experimental observation [3, 7, 14]. Those models also predict a transition to steady state creep at later times, which results from recovery.

The analysis will proceed in four steps: the first is a presentation of an infinite-dimensional phase-field model for dislocation dynamics on a single

slip plane (thought of as the 2-torus, \mathbb{T}^2). This model has been proposed by Koslowski, Cuitiño and Ortiz in [10] and a mathematically rigorous analysis of the line-tension limit can be found in [8, 9]. Secondly, this infinite-dimensional evolution will be reduced to a finite-dimensional one that takes account of the values of the phase field at certain “obstacle sites”. Thirdly, a mean-field approximation will be derived to reduce this large finite-dimensional evolution to a one-dimensional model of the energetics-and-dissipation type analyzed earlier. It will be shown that Andrade’s $t^{1/3}$ creep law follows from the reduced model when linear hardening is assumed. Finally, numerical simulations of phase-field model for dislocation dynamics are carried out. These simulations show excellent agreement with the reduced model.

1.3.1 Derivation of the mean-field model

The simplest setting is obtained if the reference configuration of the material is given by the unit torus $\mathbb{T}^2 = [0, 1]^2$ and the potential energy of a phase-field u , which represents the amount of slip in units of the Burgers vector, is given by

$$E(s, u) := \sum_{k \in \mathbb{Z}^2 \setminus \{0\}} \frac{\mu b^2}{4} \frac{1}{1/K + d/2} |\hat{u}(k)|^2 - b \cdot s \int_{\mathbb{T}^2} u(x) dx, \quad (1.17)$$

where k is the wavenumber,

$$K := \frac{1}{1 - \nu} |k|_2 - \frac{\nu}{1 - \nu} \frac{k_2^2}{|k|_2},$$

$\hat{u}(k) := \int_{\mathbb{T}^2} e^{2\pi i x \cdot k} u(x) dx$ is the k^{th} Fourier component of u , b is the Burgers vector, s is the applied shear stress, μ is the shear modulus, ν is Poisson’s ratio and d is the interplanar distance. The first term in the energy E is invariant under translations, i.e.

$$E(s, u + u') = E(s, u) + s \cdot b u' \quad (1.18)$$

if u' is a constant field. The obstacles are assumed to be disk-like subsets $B_r(p_i) \subset \mathbb{T}^2$ where $p_1, \dots, p_n \in \mathbb{T}^2$ are the centers of the obstacles and $B_r(p_i)$ is the disk with radius $0 < r \ll 1$ and center at p_i . Typically it will be assumed that the positions p_i are random and that the phase field u is constant within each obstacle, i.e. $u(x) = \xi_i$ if $x \in B_r(p_i)$. The dissipation functional Ψ depends on the obstacles and is defined as follows:

$$\Psi(\dot{u}) = \sum_{p \in \mathcal{O}} \kappa \int_{B_r(p)} |\dot{u}(x)| dx. \quad (1.19)$$

Note that in this formulation the friction functional Ψ vanishes on an infinite dimensional set, hence the assumptions of theorem 1 are not satisfied. However, since Ψ is a weighted L^1 -norm, corollary 1 implies formally that the projection of the infinite dimensional Markov chain onto the values of the elastic field on the obstacles converges to the solution of a reduced differential equation.

This differential equation is determined by constructing the appropriate Schur complement of the elastic energy, i.e. by minimizing out the the degrees of freedom that do not experience friction. For each $\xi \in \mathbb{R}^{\mathcal{O}}$, define the reduced elastic energy by

$$E_{\text{red}}(s, \xi) := \inf \{ E(s, u) \mid u \in H^{1/2}(\mathbb{T}^2) \text{ and } u(x) = \xi_i \text{ if } x \in B_r(p_i) \}$$

and the reduced dissipative potential:

$$\Psi_{\text{red}}(\dot{\xi}) := \kappa |B_r| \sum_{p \in \mathcal{O}} |\dot{\xi}_p|.$$

Note that E_{red} is a quadratic form, i.e., there exists a matrix $G \in \mathbb{R}^{\mathcal{O} \times \mathcal{O}}$, a vector $\tau \in \mathbb{R}^{\mathcal{O}}$ and a scalar $h \in \mathbb{R}$ such that $E_{\text{red}}(s, \xi) = \frac{1}{2} \xi \cdot G \xi - (s \cdot b) \tau \cdot \xi + \frac{h}{2} (s \cdot b)^2$. The coefficients of G and τ and the value of h are random and depend on the realization of the obstacle positions. The resulting free energy is

$$F(v^*) = - \sum_{p \in \mathcal{O}} \log(\kappa^2 |B_r|^2 - (v^* \cdot e_p)^2)$$

where $e_p \in \mathbb{R}^{\mathcal{O}}$ denotes the unit dislocation over the obstacle site $p \in \mathcal{O}$. Since the number of obstacles is typically large the differential equation (1.16) is difficult to analyze. The situation simplifies when one considers the asymptotic behavior of the solutions in the limit where the number of obstacles $|\mathcal{O}|$ tends to infinity and r tends to zero such that $\kappa |\mathcal{O}| |B_r| = \sigma$.

We conjecture that if $\xi(t=0)$ is constant over the obstacles, then in the limit $\xi(t)$ remains constant, i.e. there exists a fixed function $\bar{\xi}(t) \in \mathbb{R}$ such that $\xi_p(t) \rightarrow \bar{\xi}(t)$ for each $p \in \mathcal{O}$, as r tends to 0. Moreover, there exists $\bar{\tau} \in \mathbb{R}$ such that $(G\xi - (s \cdot b)\tau) \cdot e_p$ converges to $(s \cdot b)\bar{\tau} \cdot e_p$ and thus the evolution of $\bar{\xi}$ is characterized by the the following mean-field free energy:

$$F_{\text{MF}}(\bar{v}^*) := - \log(\sigma^2 - (\bar{v}^*)^2).$$

1.3.2 Derivation of the Andrade creep law

These reduction steps yield a scalar differential equation

$$\frac{d\bar{\xi}}{dt} = \theta F'_{\text{MF}}((s \cdot b)\bar{\tau}) = \frac{2\theta\bar{\tau}}{\sigma^2 - \bar{\tau}^2}$$

with appropriate initial conditions; in order to simplify the notation it is assumed that $s \cdot b = 1$. Assume a constant applied load $\bar{\tau}$ and that the resistance is σ , with $0 \leq |\bar{\tau}| < \sigma$ — once again, this is the stability criterion (1.2). At least formally, σ may vary provided that the inequality $\sigma > |\bar{\tau}| \geq 0$ still holds, and under the additional assumption of linear strain hardening, i.e. $\sigma = \sigma_0 \bar{\xi}$, the previous equation becomes

$$\frac{d\bar{\xi}}{dt} = \frac{2\theta\bar{\tau}}{\sigma_0^2 \bar{\xi}(t)^2 - \bar{\tau}^2}. \quad (1.20)$$

Clearly, the behaviour of $\bar{\xi}(t)$ for small t will depend upon the magnitude of $\bar{\tau}$ as compared to σ_0 . However, under the assumption that the effective applied stress $\hat{\tau}$ is small in comparison to the frictional resistance $\sigma = \sigma_0 \bar{\xi}$,

$$\frac{d\bar{\xi}}{dt} = \frac{2\theta\bar{\tau}}{\sigma_0^2 \bar{\xi}(t)^2}.$$

This yields

$$\bar{\xi}(t) \approx \left(C_1 + \frac{6\theta\bar{\tau}t}{\sigma_0^2} \right)^{1/3} \sim t^{1/3} \text{ as } t \rightarrow +\infty,$$

where C_1 is a constant of integration, by the general solution

$$\frac{dy}{dt} = \frac{k\theta}{(\sigma_0\theta^\alpha y(t)^\beta)^2} \implies y(t) = \left((1+2\beta) \left(C_1 + \frac{k\theta^{1-2\alpha}t}{\sigma_0^2} \right) \right)^{\frac{1}{1+2\beta}}. \quad (1.21)$$

Thus, as illustrated by the plots of numerical solutions to (1.20) in figure 1.1, Andrade's $t^{1/3}$ creep law follows as a straightforward consequence of the limiting dynamics. Furthermore, the theory also predicts more rapid creep for larger values of the temperature-like parameter θ , as intuition would suggest.

1.3.3 Numerical simulations

This subsection describes numerical simulations of the phase-field dislocation theory proposed by Koslowski, Cuitiño and Ortiz in [10]. Proceeding to the numerical solution of the phase-field dislocation model, the slip plane is discretized in a square of 50 by 50 grid points with periodic boundary conditions and a random array of obstacles. The potential energy is computed in Fourier space following (1.17). The irreversible dislocation obstacle interactions are built into the framework developed in section 1.1 by the introduction of the incremental work function (1.4).

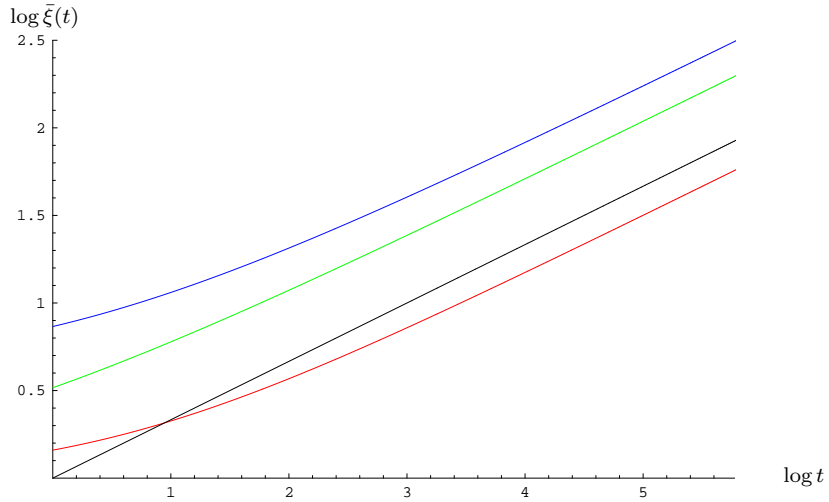


Fig. 1.1 A log-log plot of $\bar{\xi}(t)$ (colour) against t for (1.20), illustrating Andrade's $t^{1/3}$ Andrade creep law behaviour by comparison with $t \mapsto t^{1/3}$ (black). Parameters: initial condition $\bar{\xi}(0) = 1$; $\theta = 1$; $\sigma_0 = 1$; $\bar{\tau} = 0.1$ (red), 0.5 (green), 0.9 (blue).

The simulations are performed with a Metropolis Monte Carlo algorithm using the transition probability (1.4) from state u_n to u_{n+1} as derived in section 1.1.1 and the frictional potential (1.19).

Given an initial state $u_0(x)$, the phase field is set to be constant within each obstacle, i.e. $u_0(x) = \xi_i^0$ if $x \in B_r(p_i)$. The system is allowed to relax for a given applied stress $\bar{\tau}$. After the system reaches a relaxed state the values of the phase field at the obstacles points are updated with the new values. These values are used to compute the friction at the obstacles for the next time step. In the present model hardening is represented by an increase in the frictional resistance, σ following

$$\sigma = \sigma_0 \bar{u}(t)^\beta \quad (1.22)$$

where σ_0 is a hardening coefficient and \bar{u} is the average slip. Figure 1.2 shows the numerical simulations of the phase field dislocation model for different values of hardening coefficient at an applied stress $\bar{\tau} = 0.5$ and $\theta = 1$. The red line corresponds to $\beta = 0$ and shows a power law dependence on t of the form given in equation 1.21 with $\frac{1}{1+2\beta} = 0.94 \pm 0.02$.

Figure 1.2 also shows the simulations for linear hardening, i.e. $\beta = 1$. The simulated average slip follows a power law relation with respect to time with exponents $\frac{1}{1+2\beta} = 0.27 \pm 0.01$ and $\frac{1}{1+2\beta} = 0.28 \pm 0.01$ for hardening coefficients $\sigma_0 = 1$ and $\sigma_0 = 2$ respectively, in agreement with Andrade creep.

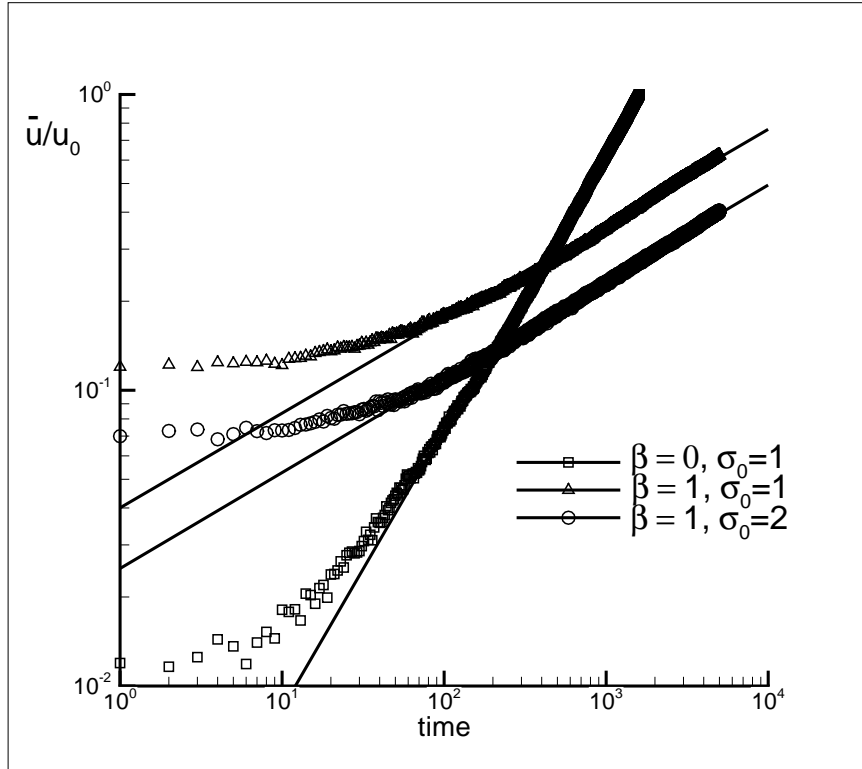


Fig. 1.2 A log-log plot of $\bar{u}(t)/u_0$ (third from top) against t . Numerical simulations of the phase-field dislocation model with no hardening (bottom), and linear hardening with $\sigma_0 = 1$ (second from top) and $\sigma_0 = 2$ (top).

1.4 Summary and conclusion

We have developed a theory of statistical mechanics for dissipative systems governed by equations of evolution that assigns probabilities to individual trajectories of the system. The theory can be made mathematically rigorous and leads to precise predictions regarding the behavior of dissipative systems at finite temperature. Such predictions include the effect of temperature on yield phenomena and rheological time exponents. The particular case of an ensemble of dislocations moving in a slip plane through a random array of obstacles has been studied numerically in detail. The numerical results bear out the analytical predictions regarding the mean response of the system, which exhibits Andrade creep.

This finite-temperature "phase-space exploration" is expected to be most revealing when the energy landscape of the system is rough and the system tends to develop microstructure (cf, e. g., [11], [4]). Of particular interest are

continuum systems whose states are described by fields in infinite-dimensional functional spaces and governed by energy functionals lacking lower semi-continuity. In such cases, the preferred or most likely trajectories may be viewed as defining the effective or macroscopic energetics and kinetics of the system.

References

1. Edward N. da C. Andrade. *Proceedings of the Royal Society of London*, A(84):1, 1910.
2. Edward N. da C. Andrade. *Proceedings of the Royal Society of London*, A(90):329, 1914.
3. Daryl C. Chrzan and M. J. Mills. Criticality in the plastic deformation of Ni_3Al . *Physical Review Letters*, 69(19):2795–2798, 1992.
4. S. Conti and M. Ortiz. Minimum principles for the trajectories of systems governed by rate problems. *Journal of the Mechanics and Physics of Solids*, 56(5):1885–1904, 2008.
5. Alan H. Cottrell. Criticality in andrade creep. *Philosophical Magazine A*, 74(4):1041–1046, 1996.
6. Alan H. Cottrell. Strain hardening in andrade creep. *Philosophical Magazine Letters*, 74(5):375–379, 1996.
7. Glenn S. Daehn. Primary creep transients due to non-uniform obstacle sizes. *Materials Science and Engineering*, A(319-321):765–769, 2001.
8. Adriana Garroni and Stefan Müller. Γ -limit of a phase-field model of dislocations. *SIAM J. Math. Anal.*, 36(6):1943–1964 (electronic), 2005.
9. Adriana Garroni and Stefan Müller. A variational model for dislocations in the line tension limit. *Arch. Ration. Mech. Anal.*, 181(3):535–578, 2006.
10. Marisol Koslowski, Alberto M. Cuitiño, and Michael Ortiz. A phase-field theory of dislocation dynamics, strain hardening and hysteresis in ductile single crystals. *J. Mech. Phys. Solids*, 50(12):2597–2635, 2002.
11. A. Mielke and M. Ortiz. A class of minimum principles for characterizing the trajectories and the relaxation of dissipative systems. *ESAIM: Control, Optimisation and Calculus of Variations*, 14:494516, 2008.
12. Alexander Mielke and Florian Theil. On rate-independent hysteresis models. *NoDEA Nonlinear Differential Equations Appl.*, 11(2):151–189, 2004.
13. Alexander Mielke, Florian Theil, and Valery I. Levitas. A variational formulation of rate-independent phase transformations using an extremum principle. *Arch. Ration. Mech. Anal.*, 162(2):137–177, 2002.
14. M. C. Miguel, A. Vespignani, M. Zaiser, and S. Zapperi. Dislocation jamming and Andrade creep. *Physical Review Letters*, 89(16):165501–1–4, 2002.
15. Michael Ortiz and Eduardo A. Repetto. Nonconvex energy minimization and dislocation structures in ductile single crystals. *Journal of the Mechanics and Physics of Solids*, 47(2):397–462, 1999.
16. Michael Ortiz and Laurent Stainier. The variational formulation of viscoplastic constitutive updates. *Computer Methods in Applied Mechanics and Engineering*, 171(3-4):419–444, 1999.
17. Raúl A. Radovitzky and Michael Ortiz. Error estimation and adaptive meshing in strongly nonlinear dynamic problems. *Computer Methods in Applied Mechanics and Engineering*, 172(1-4):203–240, 1999.
18. Tim Sullivan, Marisol Koslowski, Florian Theil, and Michael Ortiz. Dissipative systems in contact with a heat bath: Application to andrade creep. *To appear in J. Mech. Phys. Solids*, 2009.